Recent Advances in Techniques for Porosity Characterization of Membranes

Akshaya Jena and Krishna Gupta
Porous Materials, Inc
20 Dutch Mill Road, Ithaca, New York 14850
USA

Abstract

Four novel techniques developed for pore structure characterization of membranes have been discussed. Results obtained using these techniques have been presented and critically examined. The unique features of the techniques have been considered and the techniques have been compared with some of the existing ones.

Introduction

Many novel metallic, polymeric, and ceramic membranes with unusual characteristics are currently being manufactured to meet the growing demands of modern technology. Some of these membranes can even be thin and fragile. The performance of these membranes is often primarily governed by their pore structure characteristics. A specific application determines the pore structure characteristics of membranes relevant and important for that application. Special techniques are required to characterize some of the properties of membranes. In this presentation, several novel techniques are discussed for measurement of some of the unique characteristics of membranes and application of these techniques are critically examined.

Pore Diameter, Distribution and Permeability of Membranes

In many applications, membranes act as barriers to particles or organisms. The barrier characteristics of membranes are determined by their pore throat diameters and pore distributions. The rate of the separation process is governed by the rate of fluid flow through the membrane. The fluid flow rate is determined by the permeability of the membrane. The membranes are often thin, fragile and deformable. The novel technique flow porometry has been developed to characterize these relevant pore structures of membranes without distorting the pore structure.

Technique: Advanced Flow Porometry

Principle: The sample of the membrane is soaked in a wetting liquid that fills the pores spontaneously. The pressure of a non-reacting gas on one side of the sample is gradually increased to empty the pores and allow gas to flow through the sample. The differential pressure needed to empty a pore is determined by pore diameter [1].

$$p = 4 \gamma \cos \theta / D \qquad (1)$$

where,
p= differential pressure on the sample
γ = surface tension of the wetting liquid
θ = contact angle of the wetting liquid on the sample
D= pore diameter. Pore diameter is defined as the diameter of a cylindrical opening such that perimeter to area ration of the pore is the same as that of the opening.
The differential pressures and gas flow rates through wet and dry samples are measured (Figure 1).

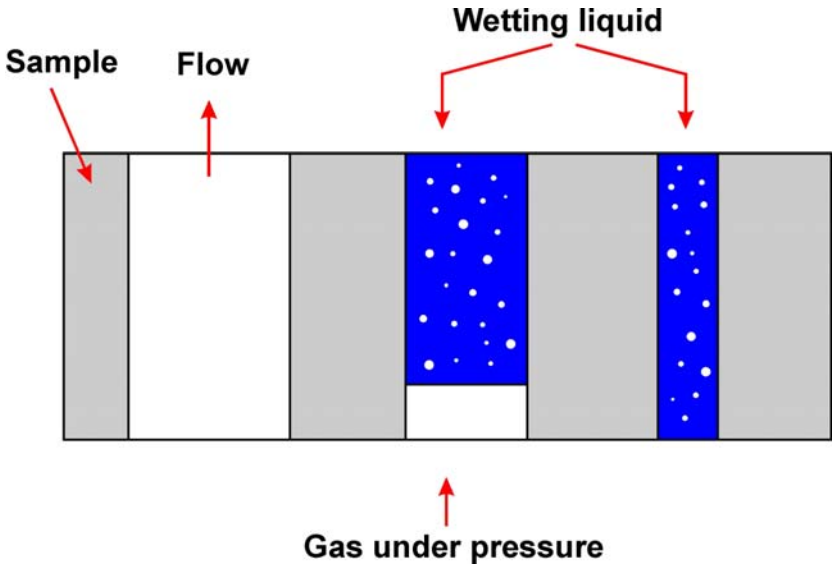

Figure 1. Illustration of the principle of capillary flow porometry

Figure 2 illustrates the characteristics of the membrane obtainable from the measured gas flow rates and differential pressures. The half-dry curve in the figure is calculated from the dry curve so as to give half of the flow rate of the dry curve at a given differential pressure.

.

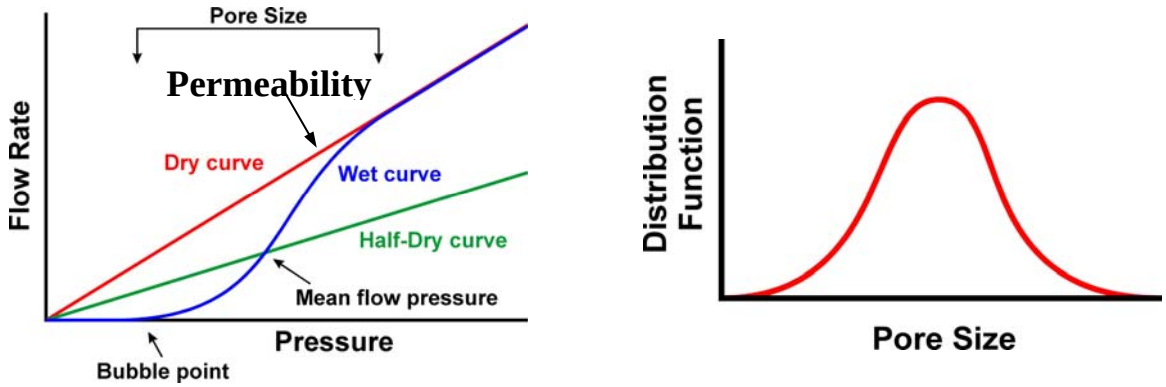

(a) Pore diameter and permeability (b) Pore distribution

Figure 2. Characteristics measurable by capillary flow porometry

Instrument: The PMI Flow Porometer that was used in this study is shown in Figure 3. The instrument uses state-of-the-art components, has many innovative designs and uses windows

based software for ease of operation. The instrument has a built in internal computer for complete automation of its operations (Figure 4). Data acquisition, data storage and data reduction in many formats are automatically performed.

Figure 3. The PMI Capillary Flow Porometer

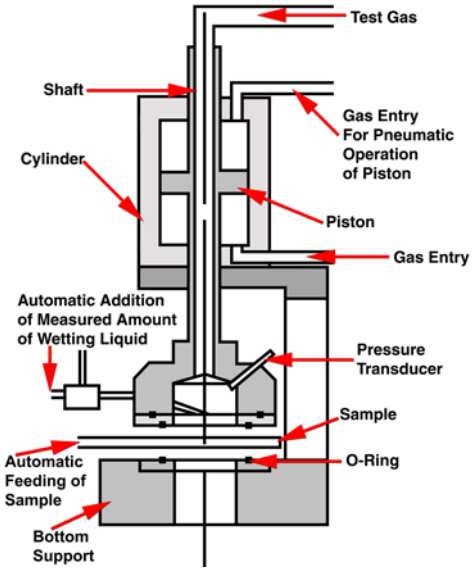

Figure 4. Schematic of complete automation incorporated in some of the advanced porometers

Accuracy and Reproducibility: In order to test the accuracy of the instrument, diameters of circular pores etched in stainless steel discs and polycarbonate membranes were measured by Scanning Electron Microscopy and capillary flow porometry. The results shown in Table 1 demonstrate the exceptional accuracy of results obtainable by the PMI Capillary Flow Porometer.

Table 1. Pore diameters measured by SEM and PMI Capillary Flow Porometer

Material	SEM Pore diameter, μm	PMI Capillary Flow Porometer Pore diameter, μm
Stainless steel disc	81.7 ± 5.2	86.7 ± 4.1
Polycarbonate membrane	4.5 ± 0.5	4.6 ± 0.1

The high reproducibility of results obtained with the PMI Capillary Flow Porometer has been demonstrated by repeating measurements up to 32 times. The results in Table 2 demonstrate the reproducibility.

Table 2. Scatter in the largest pore diameters obtained from 32 repeated measurements.

Material	Scatter in pore diameter using wetting liquid: Porewick	Silwick
Stainless steel disc	1.8 %	1.2 %
Nonwonen fibrous mat	0.2 %	1.5 %
Paper	1.7 %	1.1 %

Application

Typical gas flow rates and differential pressures measured for a membrane are shown in Figure 5. By considering free energy balance, the relation between measured differential pressures and pore diameter can be derived (Equation 1). Measured differential pressures and flow rates yield all the pore structure characteristics.

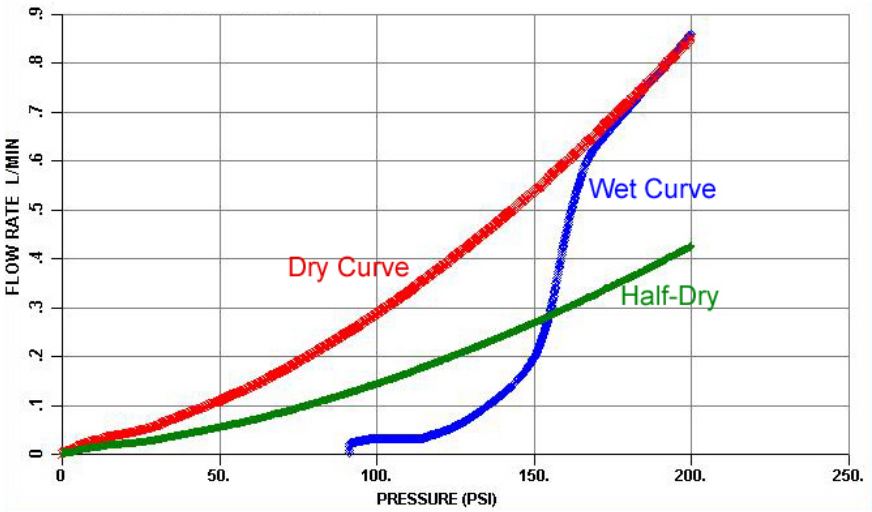

Figure 5. Change of flow rate with differential pressure for membrane #4.

Constricted pore diameter: The pores normally have irregular cross-sections and pore diameters change along pore path. The presence of a pore is detected by flow porometry when liquid is removed from the pore and gas starts flowing through the pore. Maximum pressure is needed to remove liquid from pore throat. When this maximum pressure is reached, the liquid is completely removed from the pore, gas starts flowing through it and the presence of the pore is detected. Thus, pore diameter calculated from the differential pressure at which the pore is detected is the diameter of the pore at its most constricted part. Capillary flow porometry is the only technique that is capable of measuring the constricted pore diameter that determines the barrier characteristics of a pore.

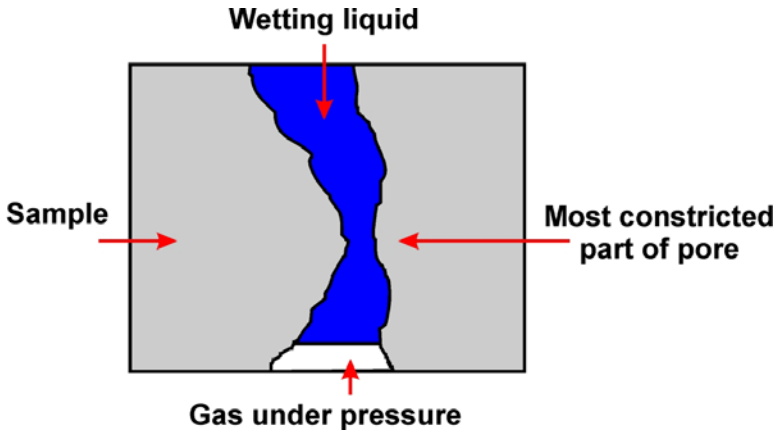

Figure 6. The pore throat diameter measured

The largest pore diameter (Bubble point pore diameter): The pressure at which gas begins to flow through the wet sample yields the largest pore diameter or the bubble point. The data in Figure 7 illustrates the procedure. The data on four membranes are listed in Table 3. Pore diameters in the range of 0.073 – 27.123 μm were easily measurable.

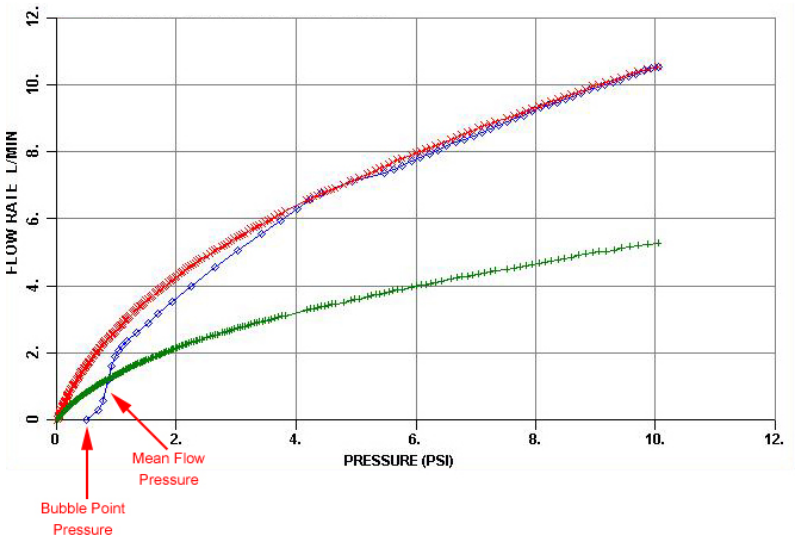

Figure 7. Variation of flow rate with pressure for membrane #3 showing bubble point pressure and mean flow pressure

Table 3. Bubble point and mean flow pore diameters of four membranes

Membrane	Bubble point pore diameter, μm	Mean flow pore pore diameter, μm
Membrane, #1	27.123	14.714
Membrane #2	17.914	3.812
Membrane #3	13.544	7.668
Membrane #4	0.073	0.043

The mean flow pore diameter: The mean flow pore diameter is computed from the mean flow pressure corresponding to the point of intersection of the wet curve and the half-dry curve. Mean flow pore diameter is such that 50 % of the flow through dry sample is through pores larger than the mean flow pore. Figure 7 illustrates the procedure. The results are listed in Table 3.

Flow distribution over pore diameter : The flow distribution is given in terms of the distribution function, f.

$$f = - d [(F_w / F_d)\times 100] / d D \qquad (2)$$

where $(F_w / F_d)_p$ is the ratio of flow through wet and dry samples at the same differential pressure. Figures 8 gives the distributions in two membranes. The distribution function is such that the flow through pores in a given range is given by the area under the curve in the same range. Membrane #1 has a single sharp peak. Most of the pore diameters are close to the mean flow pore diameter.

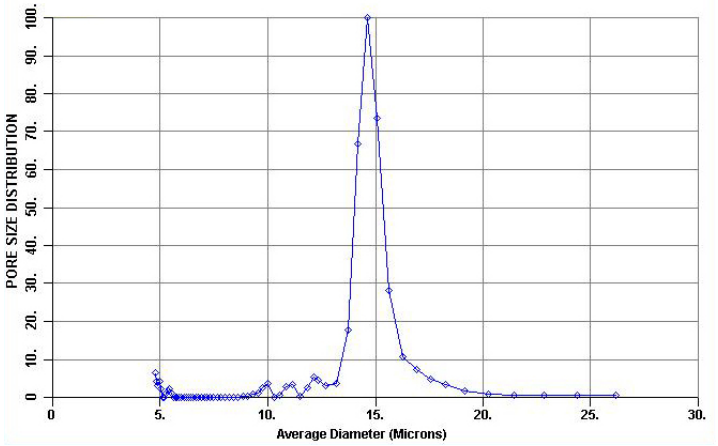

Figure 8. Pore size distribution for membrane #1

Cumulative flow distribution: The percentage cumulative flow defined as $100\times(F_w/F_d)_p$ is shown in Figures 9 for membranes, #2. The pore distribution characteristics are also clear from the cumulative flow. The membrane shows a bimodal distribution.

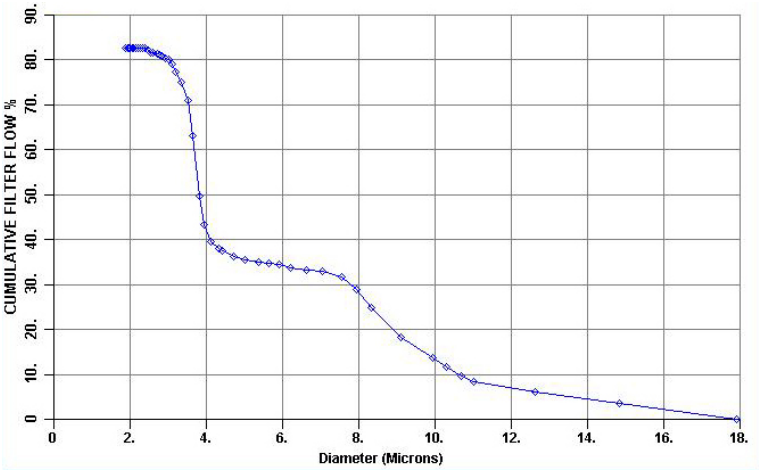

Figure 9. Cumulative flow distribution membrane #2

Gas permeability, liquid permeability and envelope surface area: Gas permeability in any desired commercial unit is computed from the dry curve. The instrument can be fitted with suitable attachments so that liquid permeability is also measurable. Gas flow rate is related to surface area, because it offers resistance to the flow of gases through porous media. The gas flow rate is used to compute the surface area of through pores.

Effects of application environment: During application, the membrane may be subjected to elevated temperatures, pressures, aggressive chemical environments, compressive stresses, and cyclic compression. Therefore, the pore structure in the application is likely to be different from that measured in the laboratory environment. The capillary flow porometer has the ability to test under simulated application conditions.

Unique Features

1. High pressures are not required. Chance of the sample getting damaged is very small.
2. Minimal sample damage and pore structure distortion.
3. No toxic material is used.
4. No special and expensive gases or gas mixtures are required.
5. Completely automated test execution, data acquisition, data storage and data reduction.
6. This technique measures only the through pores or flow pores and throat diameters.
7. Has the ability to test samples under simulated service conditions.

Characterization of Hydrophobic Pores in Membrane

The pore volume of membranes is an important characteristic for some applications. Mercury Porosimetry is often used to measure pore volume. However, this technique uses highly toxic mercury as the intrusion liquid. Also the use of high pressure can destroy the integrity of the membrane. An innovative technique has been developed to measure pore volume with water as the intrusion liquid. The technique is applicable to all hydrophobic membranes.

Technique- Water Intrusion Porosimetry (Aquapore)

Principle: A non-wetting liquid does not fill the pores spontaneously. Water is non-wetting to hydrophobic membranes. Therefore, pressure is required to force water into pores of hydrophobic membranes. The pressure on water and the volume of water that intrudes into pores are measured. The principle is illustrated in Figure 10.

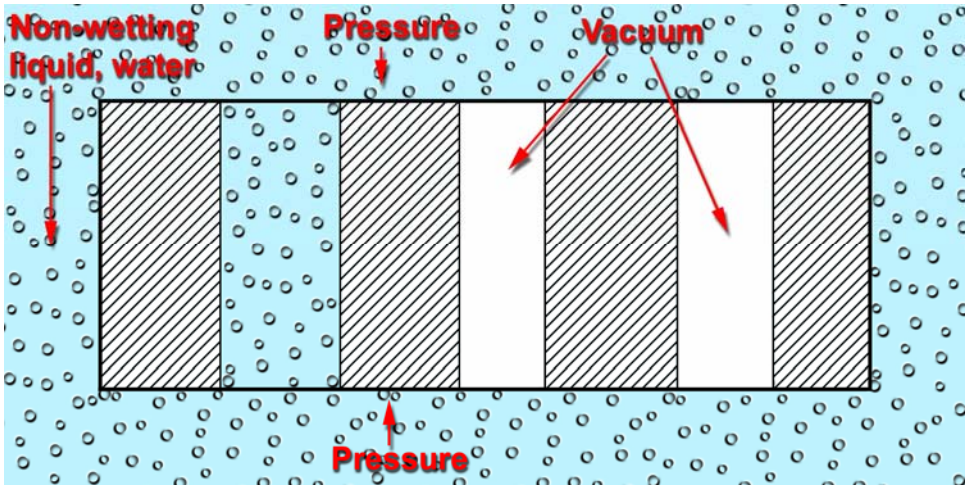

Figure 10 Principle of water porosimetry

The following relation relates pressure to pore diameter [2].

$$D = - 4 \gamma \cos \theta / p \qquad (3)$$

where:
D= pore diameter
γ = surface tension of water
θ = contact angle of water
p = differential pressure.
The contact angle of non-wetting liquids is greater than 90 and cos θ is negative. Therefore, the negative sign on the right side of Equation 3 yields positive pore diameters. Experimental data are used to compute pore diameter, pore volume and pore volume distributions.

Equipment: The PMI Water Intrusion Porosimeter is shown in Figure 11. It is a fully automated instrument that requires very little operator involvement.

Figure 11. The PMI Water Intrusion Porosimeter

Applications

Principle: The cumulative pore volume of a membrane determined in the PMI Water Intrusion porosimeter is shown in Figure 12. The pressure required was only about 1000 psi for pore diameters down to about 0.01 microns.

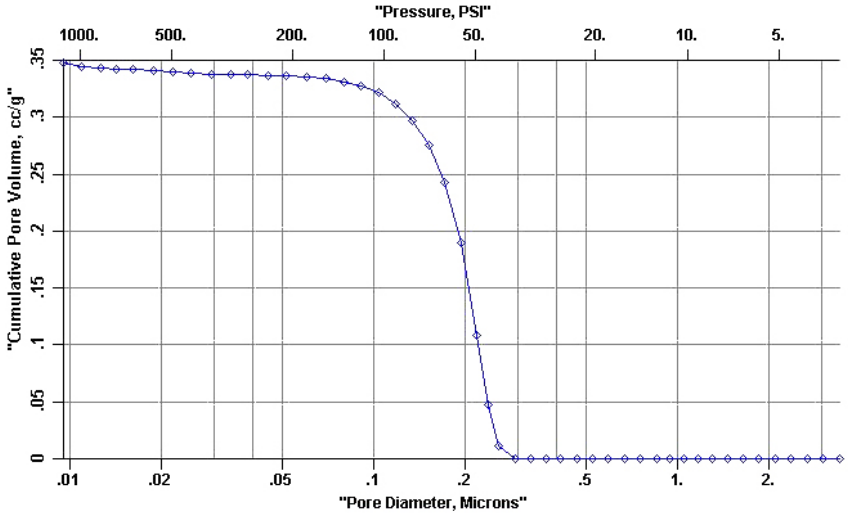

Figure 12 Change of cumulative pore volume with pore diameter

The pore volume distribution is given in Figure 13. The distribution function in this figure is defines as [-(dV/d log D)], where V is the pore volume. The area under the curve in a pore size range yields volume of pores in that range. The distribution function is maximum at about 0.22 microns

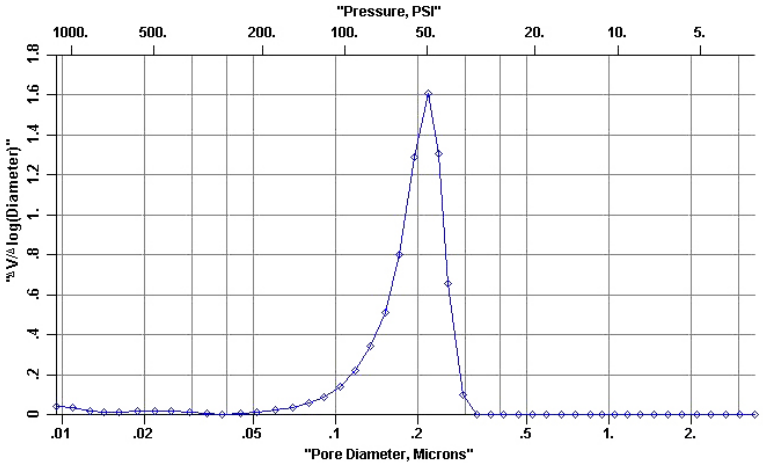

Figure 13. Pore volume distribution by water intrusion porosimetry.

Comparison with Mercury porosimetry: The results obtained with mercury intrusion porosimetry are shown in Figures 14 and 15.

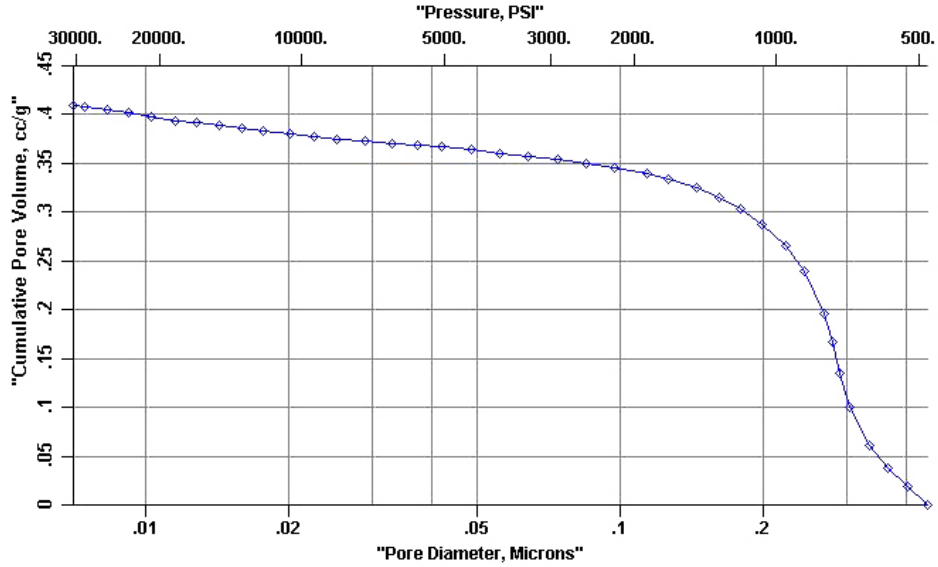

Figure 14. Cumulative pore volume measured in mercury intrusion porosimetry.

The shapes of the intrusion volume curves are similar. The intrusion volumes are similar. However, toxic mercury was used in the test and the pressure required was close to 20000 psi compared with 1000 psi required by water porosimetry.

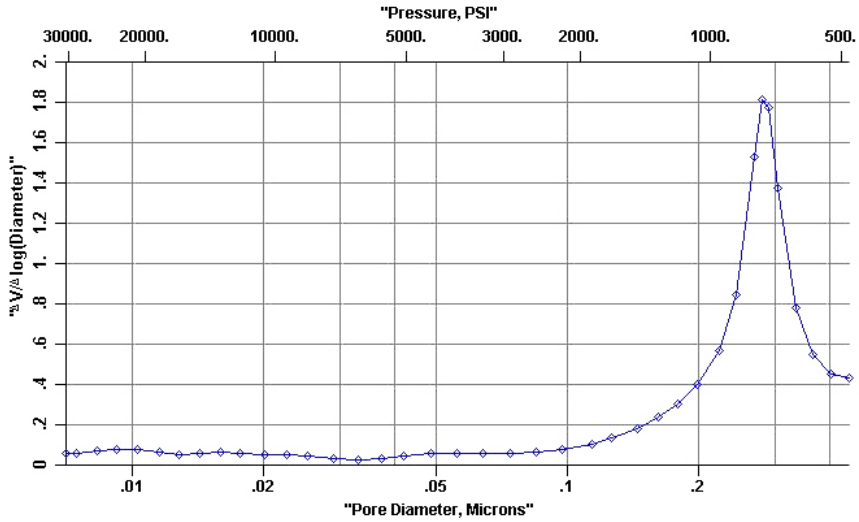

Figure 15. Pore volume distribution obtained using mercury porosimetry

The pore volume distribution curves are also similar. Both techniques give only one sharp peak. The peak in the distribution curve occurs at about 0.27 microns

Unique Features

1. No toxic substance is used.
2. Pressure required is low.
3. Minimal distortion of pore structure.
4. Smaller pores can be measured.
5. Any nonmercury nonwetting liquid of interest can be used.
6. Minimal operator involvement and completely automated test execution, data acquisition, data storage and data reduction.

Gas And Vapor Transmission Rate Through Nearly Impermeable Membranes

Gas, vapor or water vapor transmission rates through membranes have become very important for many applications in fuel cell, external wear, defense and other related industries. A number of modern membranes are almost completely impermeable to gas, but are permeable to water vapor. A novel technique has been developed to characterize some of these unusual properties of membranes.

Technique - Diffusion Permeametry

Principle: The sketch in Figures 16 illustrates the principles of the instrument. For performing a test, the sample is loaded and the instrument is evacuated. Gas or vapor is introduced on one side of the sample chamber. The pressure of the fluid is maintained at a constant value and increase in pressure on the other side is accurately measured. In order to obtain utmost accuracy the system is maintained at a constant temperature. Flow rates through the sample are computed from the rates of pressure increase [3].

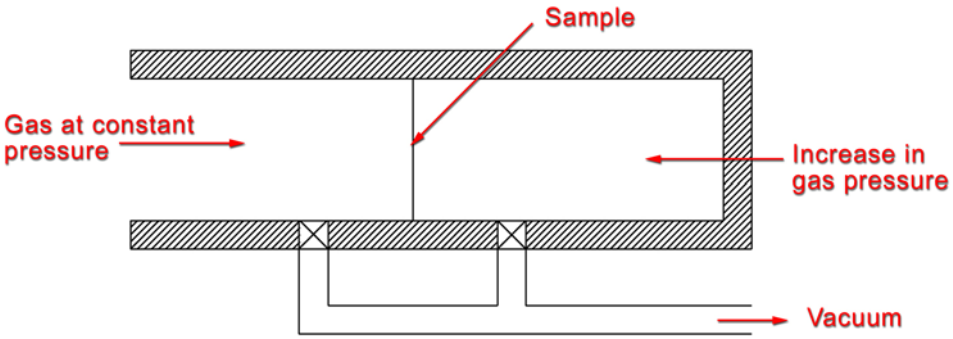

Figure 16. Principle of diffusion permeameter

Instrument: The instrument is shown in Figures 17. It is completely automated and requires very little operator involvement. For ease of operation, windows based software is used for data acquisition and reduction.

The instrument is capable of accurately measuring very small increments in pressure so that, flow rates low as 10^{-4} cm^3/s can be detected. Tests can be performed at any desired temperature up to 800 C. A number of gases and vapors can be tested. The pressures can be varied over a wide range.

Figure 17. The PMI Diffusion Permeameter

Applications

Gas Permeation: The pressure rise on the outlet side of samples of two membranes was measured. The data presented in Figure 18 demonstrate that the instrument was sensitive enough

to measure the small increment in pressure. However, these pressure increments correspond to almost negligible flow rates of gas through the membrane. These experiments confirmed that the membrane is almost impermeable to gas.

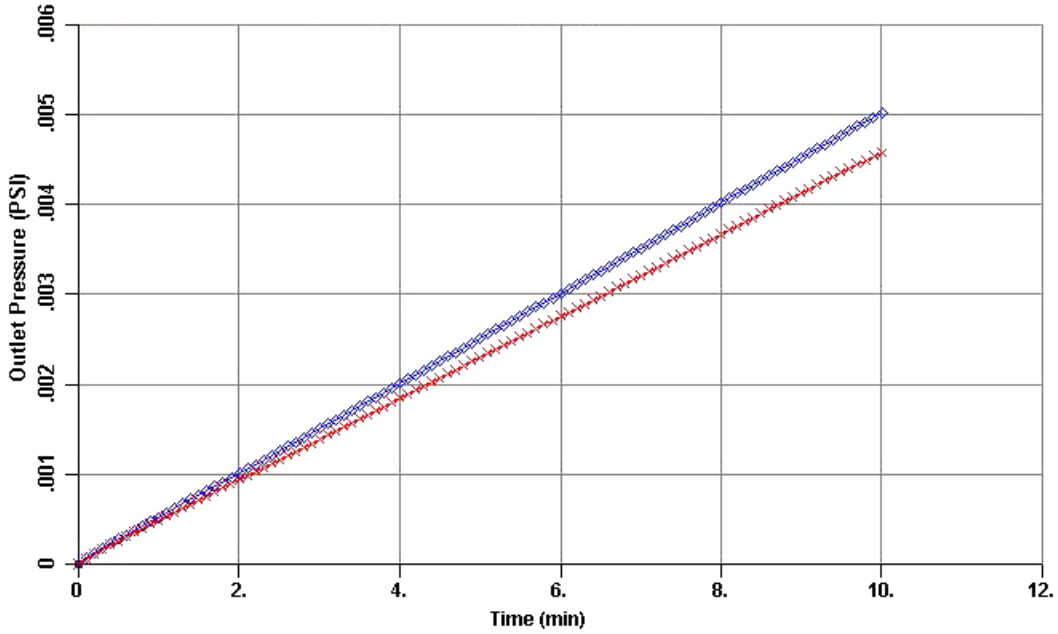

Figure 18. Change of outlet gas pressure with time for two membranes measured in the PMI Diffusion Permeameter.

Vapor permeation: The water vapor transmission rate through a nafion membrane was determined by measuring the pressure rise of water vapor on the outlet side of the sample is shown in Figure 19.

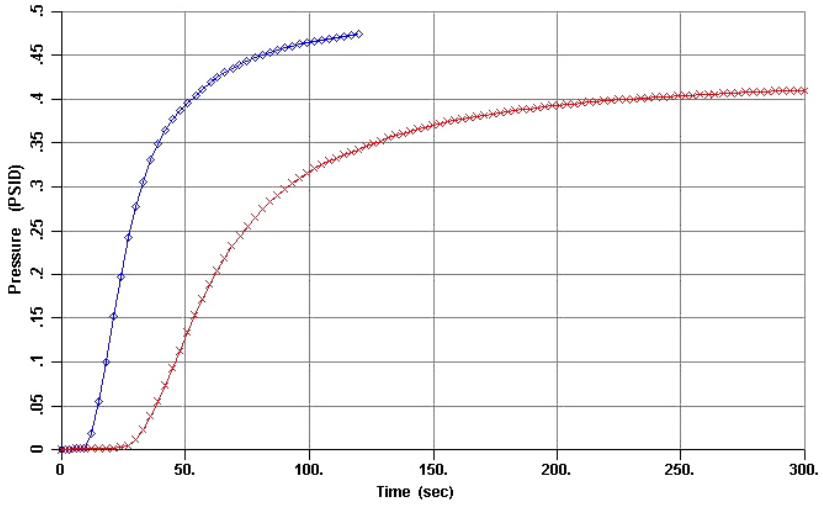

Figure 19. Change of pressure on the outlet side of two samples of the membrane in the PMI Diffusion Permeameter

The variation of pressure with time is almost sigmoidal. An incubation period is observed at the beginning. During the incubation period the pressure does not increase on the outlet side of the sample. After the incubation period, there is a small transient zone in which the pressure on

the outlet side increases with an increasing rate and then the pressure increases with a decreasing rate and approaches the constant inlet pressure of the vapor. Such behavior suggests strong interaction of vapor with the membrane.

Unique Features

1. Many gases can be tested.
2. Many vapors can be tested.
3. A wide range of test pressures can be used.
4. A wide range of test temperatures up to 800˚C can be used.
5. Very small flow rates are measurable.
6. Fully automated test execution, data acquisition, data storage and data reduction.

Water Vapor Transmission Rate Under Humidity Gradient

Technique–Water Vapor Transmission Analyzer

Principle: When a gas containing water vapor flows below as well as above a sample, vapor transport through the sample can occur due to imposed concentration, pressure or temperature gradient. Let us consider mass balance in the chamber in to which vapor is transported through the sample. Under steady state conditions, the rates of addition of water vapor by the incoming gas and by the transport through the sample must be equal to the rate of removal of water vapor by the outgoing gas (Figure 20).

$$(dn/dt) + [(p_{e,i}\phi_i / P_i) M_i = [(p_{e,o}\phi_o / P_o) M_o] \quad (4)$$

where
dn/dt = Rate of vapor transport in moles
p_e = equilibrium vapor pressure at temperature, T and total pressure, P
ϕ = humidity = (p_v/p_e)
p_v = partial pressure of vapor in unsaturated gas
M = Rate of gas flow in moles
$_i$= incoming flow
$_o$= outgoing flow
The vapor transport rate is computed from known values of T, P, ϕ, and M [4].

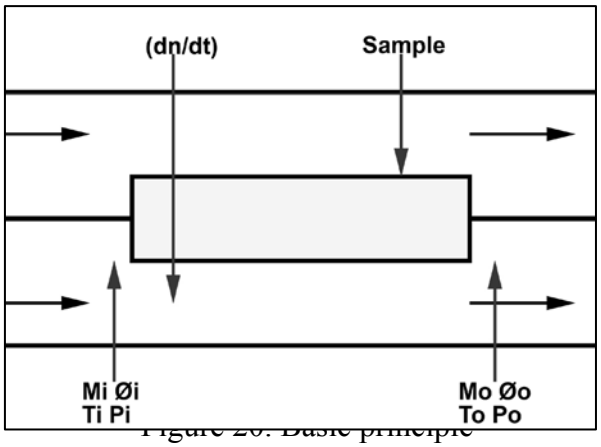

Figure 20. Basic principle

Instrument: The layout of the instrument designed for this study is shown in Figure 21. Two independent gas streams are allowed to flow on the two sides of the sample. A part of the gas flowing through each stream is allowed to go through bubblers while the other part bypasses the bubblers and mixes with the gas passing through the bubblers. For maintaining constant humidity in the inlet gas stream, the flow rate of each part of the gas stream is controlled by a flow controller utilizing a feedback circuit. It was possible to maintain humidity as high as 95 %. The sample holder and all the attachments are maintained at a constant temperature. The humidity of the gas streams is measured. The pressure is controlled by the valve at the end of each gas flow line and maintained at a value close to the atmospheric pressure.

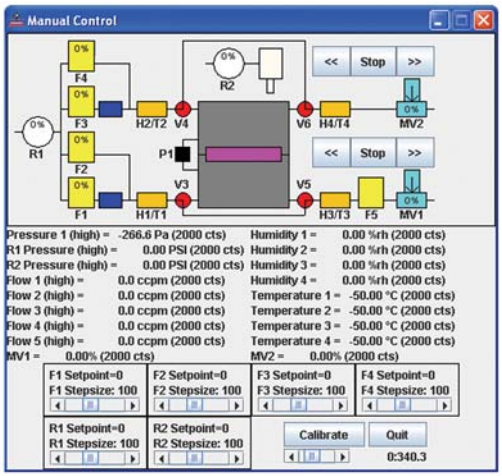

Figure 21. Layout of the measurement setup

Vapor from gas on one side of the sample diffuses through the sample and is transported to the gas on the other side. The humidity of the outgoing gas on both sides of the sample is measured. The average humidity in the incoming and outgoing gases on one side of the sample yields the average humidity on that side. The difference between the average humidity is the driving force for vapor transport.

The instrument used in this study is shown in Figure 22. The test execution, data acquisition, data storage, and data reduction are completely automated. The instrument yielded highly reliable and accurate data.

Figure 22. The PMI Water Vapor Transmission Analyzer

Application

Water vapor transmission rates were measured under humidity difference of about 0.5 maintained across the sample. Average of the humidity on the two sides of the sample was taken as the average humidity.

Plastic sheet: For evaluation of the instrument water vapor transmission rate of a plastic sheet having very low porosity was measured. The data Table 4 show the expected very small transmission rate of about 10^{-7} kg/m^2-s. The small variation of transmission rate with humidity was also detected.

Table 4. Water vapor transmission rate through a plastic sheet of very low porosity

Relative humidity, %			Flux of water vapor, kg/m^{2}s
Top	Bottom	Average	
55	5	30	2.81 E-07
65	15	40	5.99 E-07
75	25	50	4.87 E-07
85	35	60	7.60 E-07
95	45	70	1.27 E-06

Other materials: A number of samples including those of carbon filters, cathode components, diapers, and nonwovens having a wide range of transmission rates were tested (Figure 23). Water vapor transmission rates of the samples changed over a wide range and the variations of some samples with humidity were complex.

Carbon Filters: 1×10^{-4} kg/m^2-s
Cathode Component: 1×10^{-4} kg/m^2-s
Diaper: 2×10^{-5} kg/m^2-s
Nonwoven: 3×10^{-3} kg/m^2-s

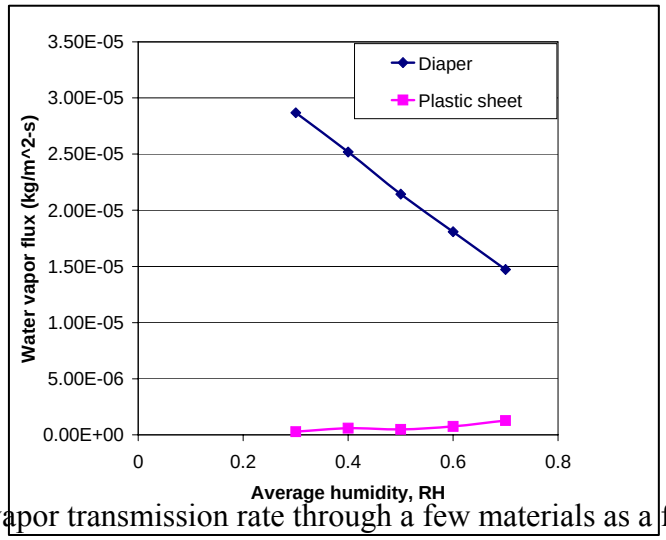

Figure 23. Water vapor transmission rate through a few materials as a function of average humidity

Unique Features

1. Any desired humidity gradient can be maintained.
2. Wide range of test temperatures is available.
3. Any desired pressure gradient can be maintained.
4. Simultaneously several gradients can be maintained.
5. No toxic material is used in the test.
6. Completely automated test execution, data acquisition, data storage and data reduction.

Summary and Conclusions

1. Four techniques developed for characterization of some of the unique properties of membranes were discussed.
2. Capillary Flow Porometry
    - Accurately measured pore diameters of membranes down to 0.073 μm. It is capable of measuring pore diameters down to several nanometers.
    - Bubble points, mean flow pore diameters, pore distributions, permeability and influence of application environments are measurable.
    - Sample was not damaged or pore structure was not distorted.
    - No toxic material was used.
3. Water Intrusion Porosimetry
    - Detected only hydrophobic pores.
    - Measured pore volume, pore diameter, and pore volume distribution.
    - Results of water intrusion porosimetry agreed well with those of mercury intrusion porosimetry.
    - No toxic material was used in the test.
    - High pressures were not required.
4. Diffusion Permeametry
    - Measured very low gas permeation rates.
    - Measured complex vapor permeation rates through nafion membrane.
    - Capable of testing at elevated temperatures and pressures.
5. Water Vapor Transmission Analyzer
    - Measured very low water vapor transmission rates.
    - Measured transmission rates over a wide range of humidity.
    - Capable of measuring transmission rates over a wide range of humidity, pressure and temperature.

References

1. Akshaya Jena and Krishna Gupta, 'Liquid Extrusion Techniques for Pore Structure Evaluation of Nonwovens', International Nonwovens Journal, Fall, 2003, pp.45-53.
2. Akshaya Jena and Krishna Gupta, 'Characterization of Pore Structure of Filtration Media', Fluid/ particle Separation Journal, Vol. 14, No. 3, 2002, pp.227-241.
3. Akshaya Jena and, Krishna Gupta, 'Characterization of Water Vapor Permeable Membranes', Desalination, Vol. 149, 2002, pp. 471- 476.

4. Akshaya Jena, Krishna Gupta, and Matthew Connolly, 'Characterization of Water Vapor Transmission Rate Through Fuel Cell Components', Fuel Cell Science, Engineering and Technology – 2004, ASME, 2004, pp. 15- 17.